Sciencexpress Report

Femtomolar Sensitivity of a NO Sensor from *Clostridium botulinum*

Pierre Nioche,[1] Vladimir Berka,[2] Julia Vipond,[3] Nigel Minton,[4] Ah-Lim Tsai,[2] C. S. Raman[1*]

[1]Structural Biology Research Center and Department of Biochemistry and Molecular Biology, [2]Division of Hematology, Internal Medicine, University of Texas Medical School, Houston, TX 77030, USA. [3]Health Protection Agency, Porton Down, Salisbury, Wiltshire SP4 0JG, UK. [4]Center of Biomolecular Sciences and Institute of Infection, Immunity and Inflammation, University of Nottingham, Nottingham NG7 2RD, UK.

*To whom correspondence should be addressed: E-mail: c.s.raman@uth.tmc.edu

Nitric oxide (NO) is extremely toxic to *Clostridium botulinum*, but its molecular targets are unknown. Here, we identify a heme protein sensor (SONO) that displays femtomolar affinity for NO. The crystal structure of the SONO heme domain reveals a novel fold and a strategically placed tyrosine residue that modulates heme-nitrosyl coordination. Furthermore, the domain architecture of a SONO ortholog cloned from *Chlamydomonas reinhardtii* indicates that NO signaling through cyclic guanosine monophosphate arose before the origin of multicellular eukaryotes. Our findings have broad implications for understanding bacterial responses to NO, as well as for the activation of mammalian NO-sensitive guanylyl cyclase.

Nitric oxide (NO) is a small, short-lived, and highly-reactive gaseous molecule. In mammals NO is biosynthesized from L-arginine by nitric oxide synthases, and it plays a key role in many and disparate cellular responses including host defense against microbial pathogens (*1*). Denitrifying bacteria generate NO (1–70 nM) by a unique mode of respiration in which nitrogen oxides (NO_3^-, NO_2^-, NO and N_2O) are reduced to N_2 (*2*). Non-denitrifiers, like *Escherichia coli*, can produce NO during anaerobic nitrate respiration ($NO_3^- \rightarrow NO_2^- \rightarrow NH_4^+$) although at much reduced levels (*3*). *Clostridium botulinum*, a strict anaerobe, is neither a denitrifier nor capable of making NO via other mechanisms. It is the etiological agent of botulism and produces the most toxic substance known to humans ($LD_{50} \approx 0.2$ ng/kg of body weight). Since the late 1920s sodium nitrite, with NO as the antimicrobial principle, has been used to inhibit the growth of heat-resistant *C. botulinum* spores and toxin production in cured meats (*4–6*). However, the molecular strategies utilized by this bacterium to recognize and avoid NO in its native and host environments have remained elusive.

To identify candidate NO sensors in *C. botulinum*, we investigated the hypothesis (*7*, *8*) that a prokaryotic counterpart to the mammalian NO receptor, soluble guanylyl cyclase (sGC) (*9*, *10*), exists and that a bacterial NO sensor may communicate with the chemotaxis machinery. Thus, we screened the genome of *C. botulinum* (http://www.sanger.ac.uk/Projects/C_botulinum/) for an ortholog of the NO-binding heme domain (*11*) of human sGC-β_1. We found a gene that encodes for a two-domain protein (598 amino acids) in which the N-terminal domain shares 15% sequence identity with the first 186 amino acids of sGC-β_1 and the C-terminal domain is similar to that of a methyl-accepting chemotaxis protein. Because the N-terminal region of mammalian sGC is indispensable for NO binding, we named the *C. botulinum* protein SONO (*sensor of NO*). RT-PCR analysis (fig. S1) (*12*) showed a transcript of the predicted size and confirmed that SONO was expressed in actively growing vegetative *C. botulinum* cells.

We overproduced its N-terminal domain (residues 1–186, CB-$SONO_{HD}$) in *Escherichia coli*. Purified CB-$SONO_{HD}$ is red in color and electronic spectroscopy revealed the presence of a *b*-type heme (*12*). Mass spectrometry confirmed the identity of the heme prosthetic group (iron protoporphyrin IX) (*13*). A heme protein has not been previously identified in *Clostridia*. To assess the coordination structure of the heme in CB-$SONO_{HD}$, we recorded its electron paramagnetic resonance (EPR) spectra (*12*). The protein yielded a classic three-line spectrum (*14*) (Fig. 1A) diagnostic of a five-coordinate (5c) low-spin heme-nitrosyl, Fe(II)(NO), complex that is unaffected by exposure to air. The main spectral feature is the 3-line hyperfine splitting centered at $g_z = 2.007$ with a separation of 1.7 mT. The splitting arises from the strong coupling between the unpaired electron spin and the nuclear spin ($I = 1$) of the ^{14}N atom of NO. It further indicates that the proximal Fe–histidine bond in the protein is readily broken. Such an air-stable heme-nitrosyl is unprecedented (*15–17*) [supporting online material (SOM) note 1]. We followed the aerobic decay of the three-line EPR signal of CB-$SONO_{HD}$ as a function of time. A $t_{1/2}$ of 70 ± 16 hours ($n = 3$) was obtained (fig. S2) and is equivalent to a dissociation rate constant (k_{off}) of $\approx 3 \times 10^{-6}$ s^{-1}. NO binding to $SONO_{HD}$ is diffusion limited [$k_{on} \approx 10^8$ M^{-1} s^{-1}, (*18*)] and we obtain an

equilibrium dissociation constant ($K_D = k_{off}/k_{on}$) of ≈ 30 × 10^{-15} M. This value approaches that suggested for NO binding to four-coordinate model heme compounds (*15*), but has not been previously reported for Fe(II)-heme proteins (SOM note 2). The presence of an air-stable Fe(II)(NO) species indicates that molecular oxygen cannot react with this complex.

We used CB-SONO$_{HD}$ to quantify the amount of NO generated during aerobic growth of *E. coli*. *E. coli* are thought to generate NO only during anaerobic nitrate respiration (*3*) because NO production is undetectable during aerobic growth [as we confirmed with chemiluminescence-based NO analyzer (Eco Physics CLD88sp) with a sensitivity <1 part per billion)]. However, the EPR spectra of intact *E. coli* cells aerobically expressing CB-SONO$_{HD}$ (Fig. 1B) resembled those of purified CB-SONO$_{HD}$ suggesting that the bound NO originated in the *E. coli* cytosol (SOM note 3). Cells that did not express CB-SONO$_{HD}$ are devoid of this signal. Quantitative EPR measurements (*12*) indicated that the *E. coli* cells produced (assuming a linear rate of formation) approximately one molecule of NO cell^{-1} min^{-1} (SOM note 4). The number of NO molecules bound to highly purified CB-SONO$_{HD}$ was in the same range as that measured from intact cells. Notice, however, that one free molecule of NO per *E. coli*, with a cell volume of 10^{-15} L (*19*), translates to a concentration of ~10^{-9} M. It is conceivable that one or more NO molecules may persist within the cytoplasm of a denitrifying cell, but this would not be true for *E. coli* which lacks the denitrification machinery (SOM note 5). Therefore, our ability to detect NO production in aerobically grown *E. coli* (*12*) is a direct consequence of CB-SONO$_{HD}$ functioning as a high-affinity sensor of NO.

We determined the crystal structure of a SONO ortholog (table S1) from the extremely thermophilic organism *Thermoanaerobacter tengcongensis*, strain MB4^T, (*20*) (SOM note 6) [TT-SONO; 39% sequence identity with CB-SONO (fig. S3)] due to difficulties in growing crystals of CB-SONO$_{HD}$. The tertiary topology of TT-SONO heme domain (TT-SONO$_{HD}$) is characterized by a proximal domain with an αββαββ motif and an α-helical distal domain (fig. S4). This fold has not been described previously. The heme is sandwiched between the two domains (Fig. 2) and its iron atom is coordinated by His^{102}. Heme recognition is mediated by hydrogen bonds between the propionates and the strictly conserved side chains of Tyr^{131}, Ser^{133} and Arg^{135} (fig. S5 and S3; SOM note 7). Numerous non-bonded contacts exist between the tetrapyrrole and the residues that form the binding pocket. With the exception of Tyr^{140}, the distal heme pocket is apolar and there are no polar atoms within 7 Å of the heme iron. During structure refinement it became clear that a distal ligand was bound to the heme iron. The protein has a Soret maximum at 416 nm which suggests the presence of a hexa-coordinate Fe(II)(O_2)complex (SOM note 8). As a consequence we modeled dioxygen into the density (Fig. 3). The chemical makeup of the TT-SONO$_{HD}$ distal heme pocket resembles that of the ThrE11Val variant (*21*) of *Cerebratulus lacteus* mini-hemoglobin (fig. S6). This protein also purifies as a high-affinity Fe(II)(O_2) complex and like TT-SONO$_{HD}$, has a Tyr residue within H-bonding distance to the terminal oxygen (SOM note 9).

Although both TT-SONO$_{HD}$ and CB-SONO$_{HD}$ have a similar constellation of side chains in the distal heme pocket (fig. S6), we have been unable to generate a stable Fe(II)(O_2)complex with CB-SONO$_{HD}$. NO-stripped CB-SONO$_{HD}$ also readily oxidizes to its Fe(III) state. Like *C. botulinum*, *T. tengcongensis* is a strict anaerobe, however, with an optimal growth temperature of 75ºC (*20*). At 70ºC TT-SONO$_{HD}$ did not form a stable Fe(II)(O_2)complex, but instead readily oxidized to the Fe(III) state. Upon addition of exogenous NO, TT-SONO$_{HD}$ also generated a five-coordinate Fe(II)(NO) complex at 70ºC. In contrast, a six-coordinate (6c) Fe(II)(NO) complex was formed at 25ºC and we found no evidence for a heme-nitrosyl complex in purified TT-SONO$_{HD}$.

To assess the role of electrostatic interactions (*22*, *23*) in stabilizing the bound ligand, we replaced the distal Tyr^{139} with a Phe in CB-SONO$_{HD}$ (fig. S6) This substitution resulted in a protein that was unable to generate a 5c-heme-nitrosyl, but instead produced a stable 6c-Fe(II)(NO) complex (fig. S7). The ability of an amino acid side chain in the distal pocket to modulate the bond strength of the proximal Fe-His linkage is unparalleled in heme protein research. Altogether, these results identify that NO binds on the distal side in CB-SONO$_{HD}$ and suggest that electrostatic interaction with Tyr^{139} is necessary for generating a neet 5c-Fe(II)(NO) complex and subsequently breaking the Fe-His bond (SOM note 10).

There appears to be a strong evolutionary pressure to modulate the NO sensitivity and specificity for SONO. For example, the rate of NO dissociation from CB-SONO$_{HD}$ is at least two orders of magnitude slower than that of sGC (*24*). To evaluate the structural basis for such variation, we used TT-SONO$_{HD}$ as a template to generate homology models of SONO$_{HD}$ from human sGCβ$_1$ and *Nostoc punctiforme* (filamentous cyanobacterium) [(NP-SONO; the full-length protein represents the heme domain and comprises amino acids 1–183 and shares 40% sequence identity with human sGCβ$_1$ (fig. S3)]. Unlike CB-SONO$_{HD}$ and TT-SONO$_{HD}$ neither human sGCβ$_1$ nor NP-SONO incorporates a Tyr side chain for interacting with the bound ligand (fig. S6). Furthermore, the distal heme pocket lacks a polar atom within 7 Å of the heme iron. Consistent with this, purified NP-SONO is characterized by a Soret maximum at 431 nm and shows no apparent EPR signal (Fig. 1C) because it contains a Fe(II) five-coordinate high-spin heme (SOM note 11). Most

heme proteins, except sGC (*25*, *26*), can maintain this state only under anaerobic conditions, for oxygen will readily bind to the sixth coordination position. However, the Fe(II)-heme of NP-SONO remains five-coordinate even after several weeks of aerobic storage at 4°C. Since fossil data show that the *Nostoc* branch of the cyanobacterial tree diverged by 2.1 Ga (billion years ago) (*27*), total exclusion of oxygen from the coordination sphere of SONO concomitant with a diminution of NO sensitivity may have occurred before the origin of unicellular eukaryotes.

To better delimit when during evolution the functional transition from SONO to sGC may have taken place, we examined the genome of *Chlamydomonas reinhardtii*—the eukaryotic unicellular green alga whose chloroplasts are derived from cyanobacteria (*28*). We found a *Chlamydomonas* EST whose product shares similarity with NP-SONO. We cloned the gene, and its product represents a full-length sGC-β with close resemblance to human sGC-β_1 (fig. S8; SOM note 12). A sGC ortholog has not been previously reported in a chloroplast-containing organism. The two proteins share similar non-polar distal heme pockets and both contain a Phe side chain in close proximity to the heme iron. Thus, eukaryotic sGC-β_1 may have evolved by the fusion of bacterial $SONO_{HD}$ and a cyclase, thereby coupling NO binding to cGMP production before the origin of animals.

In summary, we have uncovered a heme protein sensor that may be used by *C. botulinum* to recognize the presence of NO and mediate a phobic response as protective mechanism (SOM note 13). Although *C. botulinum* is a motile organism we have no direct evidence that it moves away from a source of noxious NO. However, two independent observations suggest that CB-SONO can sense and transduce signals to the chemotaxis machinery. First, the two-domain architecture of CB-SONO is reminiscent of the soluble aerotransducer HemAT (*29*) in which a myoglobin-like heme domain is used to sense O_2 and the methyl-accepting chemotaxis protein domain helps with initiating bacterial aerotaxis. Second, the gene encoding for SONO in *Vibrio cholerae* is repressed by about eight-fold alongside other chemotaxis genes in vibrios shed by cholera-infected individuals (*30*, *31*). Furthermore, we draw a parallel between the suggested taxis role for SONO in bacteria and the ability of sGC to confer chemoattractive responses to dentrites and axons (*32*). Our structural findings also provide mechanistic insights into how NO activates sGC in mammalian systems (fig. S9, S10; SOM note 14). Taken together, our studies indicate that $SONO_{HD}$, with alterations to its NO sensitivity, may have been co-opted to serve as a NO-activated molecular switch for regulating distinct cellular processes.

References and Notes

1. L. J. Ignarro, in *Nitric Oxide: Biology and Pathobiology*, L. Ignarro, Ed. (Academic Press, San Diego, 2000), pp. 3–19.
2. W. G. Zumft, *J. Mol. Microbiol. Biotechnol.* **4**, 277 (2002).
3. H. Corker, R. K. Poole, *J. Biol. Chem.* **278**, 31584 (2003).
4. D. Reddy, J. R. Lancaster Jr., D. P. Cornforth, *Science* **221**, 769 (1983).
5. R. Cammack *et al*., *Biochim. Biophys. Acta.* **1411**, 475 (1999).
6. P. M. Davidson, in *Food Microbiology: Fundamentals and Frontiers* M. P. Doyle, L. R. Beuchat, T. J. Montville, Eds. (ASM Press, Washington, DC, 2001), pp. 593–627.
7. R. J. P. Williams, *Biochim. Biophys. Acta* **1058**, 71 (1991).
8. S. J. Ferguson, *Biochim. Biophys. Acta* **1058**, 17 (1991).
9. F. Murad, *Angew. Chem. Int. Ed.* **38**, 1856 (1999).
10. D. Koesling, M. Russwurm, E. Mergia, F. Mullershausen, A. Friebe, *Neurochem. Int.* **45**, 813 (2004).
11. B. Wedel *et al*., *Proc. Natl. Acad. Sci. U. S. A.* **91**, 2592 (1994).
12. Materials and methods are available as supporting material on *Science* Online.
13. R. Timkovich, personal communication.
14. T. Yonetani, A. Tsuneshige, Y. Zhou, X. Chen, *J. Biol. Chem.* **273**, 20323 (1998).
15. T. G. Traylor, V. S. Sharma, *Biochemistry* **31**, 2847 (1992).
16. P. C. Ford, I. M. Lorkovic, *Chem. Rev.* **102**, 993 (2002).
17. G. R. Wyllie, W. R. Scheidt, *Chem. Rev.* **102**, 1067 (2002).
18. J. S. Olson, personal communication.
19. C. E. Outten, T. V. O'Halloran, *Science* **292**, 2488 (2001).
20. Y. Xue, Y. Xu, Y. Liu, Y. Ma, P. Zhou, *Int. J. Syst. Evol. Microbiol.* **51**, 1335 (2001).
21. A. Pesce *et al*., *J. Biol. Chem.* **279**, 33662 (2004).
22. G. N. Phillips, Jr., M. L. Teodoro, T. Li, B. Smith, J. S. Olson, *J. Phys. Chem.* **103**, 8817 (1999).
23. M. R. Thomas, D. Brown, S. Franzen, S. G. Boxer, *Biochemistry* **40**, 15047 (2001).
24. V. G. Kharitonov, V. S. Sharma, D. Magde, D. Koesling, *Biochemistry* **36**, 6814 (1997).
25. R. Gerzer, E. Böhme, F. Hofmann, G. Schultz, *FEBS Lett.* **132**, 71 (1981).
26. J. R. Stone, M. A. Marletta, *Biochemistry* **33**, 5636 (1994).
27. A. H. Knoll, *Science* **285**, 1025 (1999).
28. W. Martin *et al*., *Nature* **393**, 162 (1998).
29. S. Hou *et al*., *Nature* **403**, 540 (2000).
30. D. S. Merrell *et al*., *Nature* **417**, 642 (2002).
31. A. Camilli, personal communication.
32. F. Polleux, T. Morrow, A. Ghosh, *Nature* **404**, 567 (2000).

33. C.S.R. dedicates this paper to M. Perutz and T. Traylor. C.S.R. is grateful to F. Rudolph and Rice University for providing laboratory space during the 2001 Houston flood; S. Boxer, J. Eraso, P. Ford, A. Grossman, J. Groves, M.

Ikeda-Saito, J. Linder, W. Martin, J. Meeks, J. Olson, T. Poulos, F. Robb, J. Schrager, J. Schultz, J. Shapleigh, T. Spiro, S. Veeraraghavan, F.A. Walker, and W. Zumft for stimulating discussions; A. Camilli, J. Kaper, J. Olson, N. Stokes, R. Timkovich, T. Tomita, and B. Weiss for communicating unpublished results; C. Churcher, E. Harris, J. Kropat, T. McKarns, J. Meeks, S. Merchant, F. Murad, J. Parkhill, I. Scott, Eco Physics, Japanese Collection of Microorganisms, and Kazusa DNA Research Institute for access to strains, genomic DNA, RNA, protocols, and instrumentation; G. Bricogne for providing BUSTER and C. Vonrhein for assistance with using the program; and the Advanced Light Source (beamline 8.3.1, J. Holton, J. Tanamachi), Stanford Synchrotron Radiation Laboratories (beamline 9.2, M. Soltis), and European Synchrotron Radiation Facility (beamline ID29, W. Shepard) for beam time. This work is supported by the Pew Charitable Trusts through a *Pew Scholar Award* (C.S.R.), The Robert A. Welch Foundation grant AU-1524 (C.S.R.), National Institutes of Health grant R01 AI054444 (C.S.R.), and Association pour la Recherche sur le Cancer (P.N.). The GenBank accession number for *C. reinhardtii* sGC-β cloned in this work is AY343540. Coordinates and structure factors are available from the RCSB Protein Data Bank under accession code 1XBN.

Supporting Online Material

www.sciencemag.org/cgi/content/full/1103596/DC1
Materials and Methods
Figs S1 to S10
Table S1
References and Notes

3 August, 2004; accepted 27 September, 2004
Published online 7 October 2004; 10.1126/science.1103596
Include this information when citing this paper.

Fig. 1. EPR spectra of SONO heme domain ($SONO_{HD}$). (**A**) CB-$SONO_{HD}$ purifies as a heme-nitrosyl complex. (**B**) *E. coli* cells overproducing CB-$SONO_{HD}$. (**C**) Purified NP-SONO. (Sidebar) Coomassie-stained SDS-PAGE gel. The relative molecular sizes of NP- and CB-$SONO_{HD}$ are 22,482, and 22,630, respectively.

Fig. 2. Three-dimensional structure of TT-$SONO_{HD}$. Ribbon diagram depicts residues 1–181 of the protein. The heme prosthetic group (red) and the histidine coordinating its iron are also shown.

Fig. 3. Omit difference electron density map ($F_{obs} - F_{calc}$) of the heme pocket. Maps are shown at 3σ level. Oxygen ligand density is in blue. Dotted line indicates that the phenolic –OH of Tyr^{140} is within H-bonding distance of the oxygen ligand.

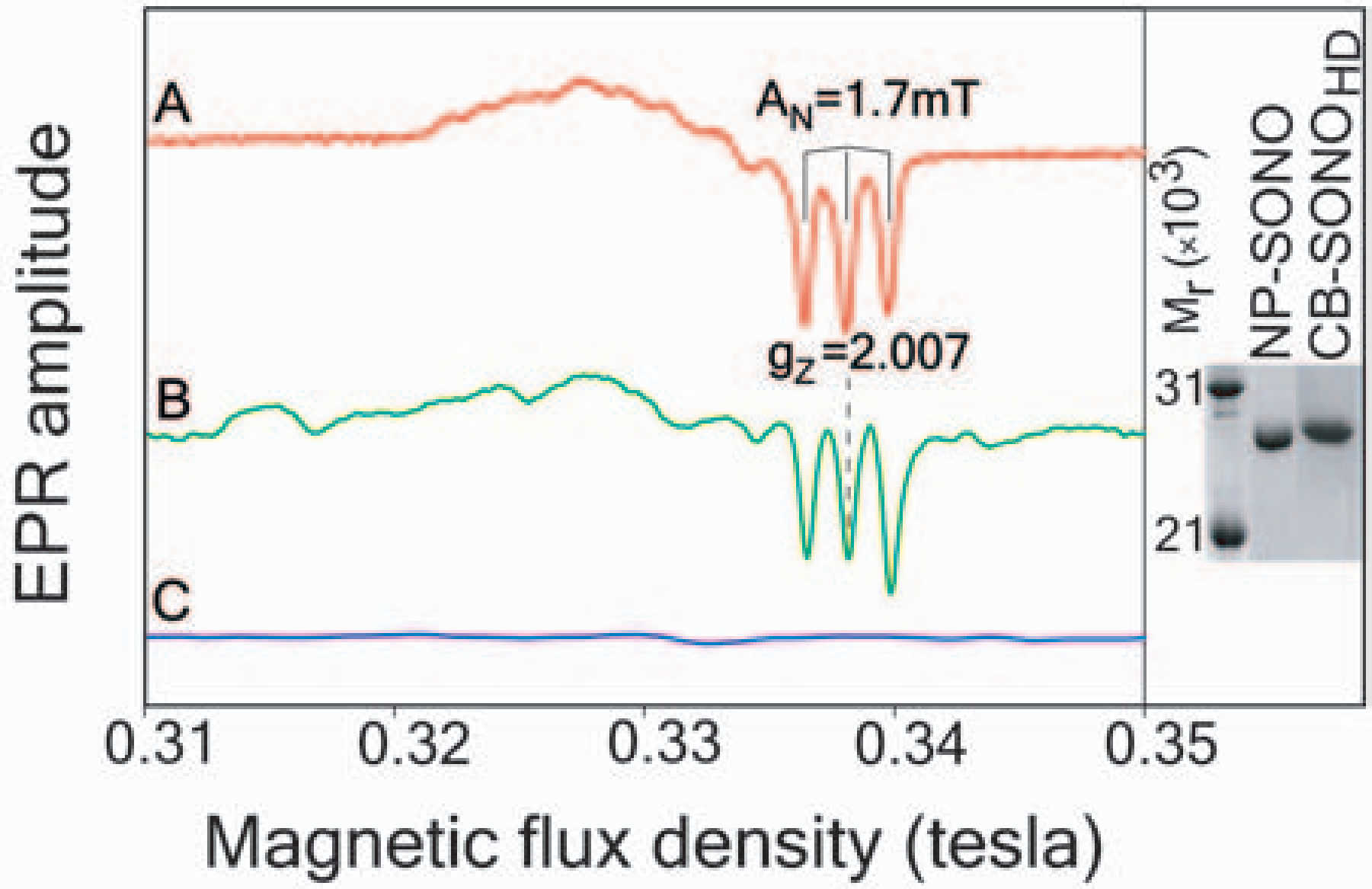
A
B
C
A_N=1.7mT
g_Z=2.007
EPR amplitude
0.31
0.32
0.33
0.34
0.35
Magnetic flux density (tesla)
M_r ($\times 10^3$)
31
21
NP-SONO
CB-SONO^{HD}

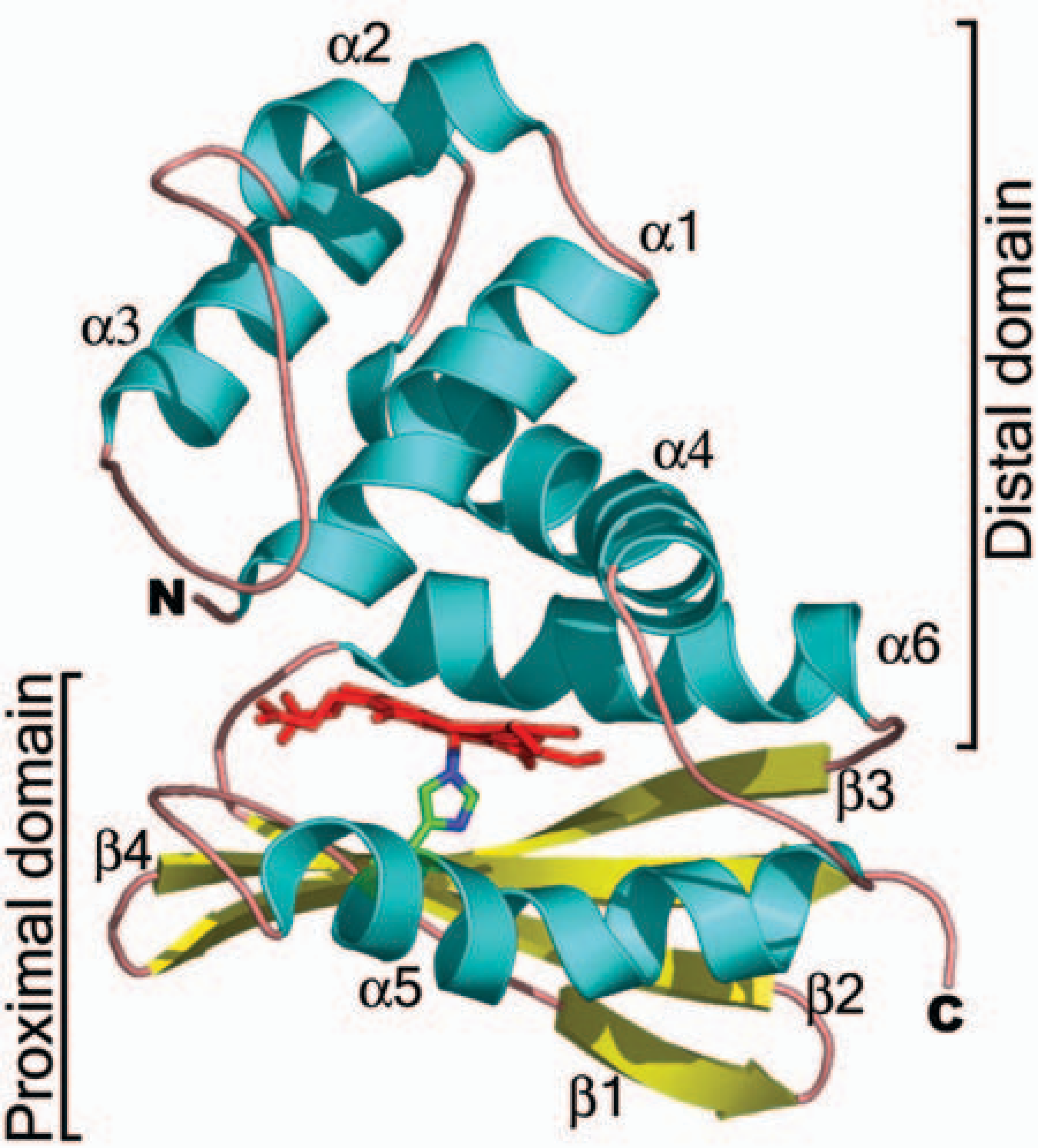
α2
α1
α3
α4
N
α6
Distal domain
Proximal domain
β3
β4
α5
β2
C
β1

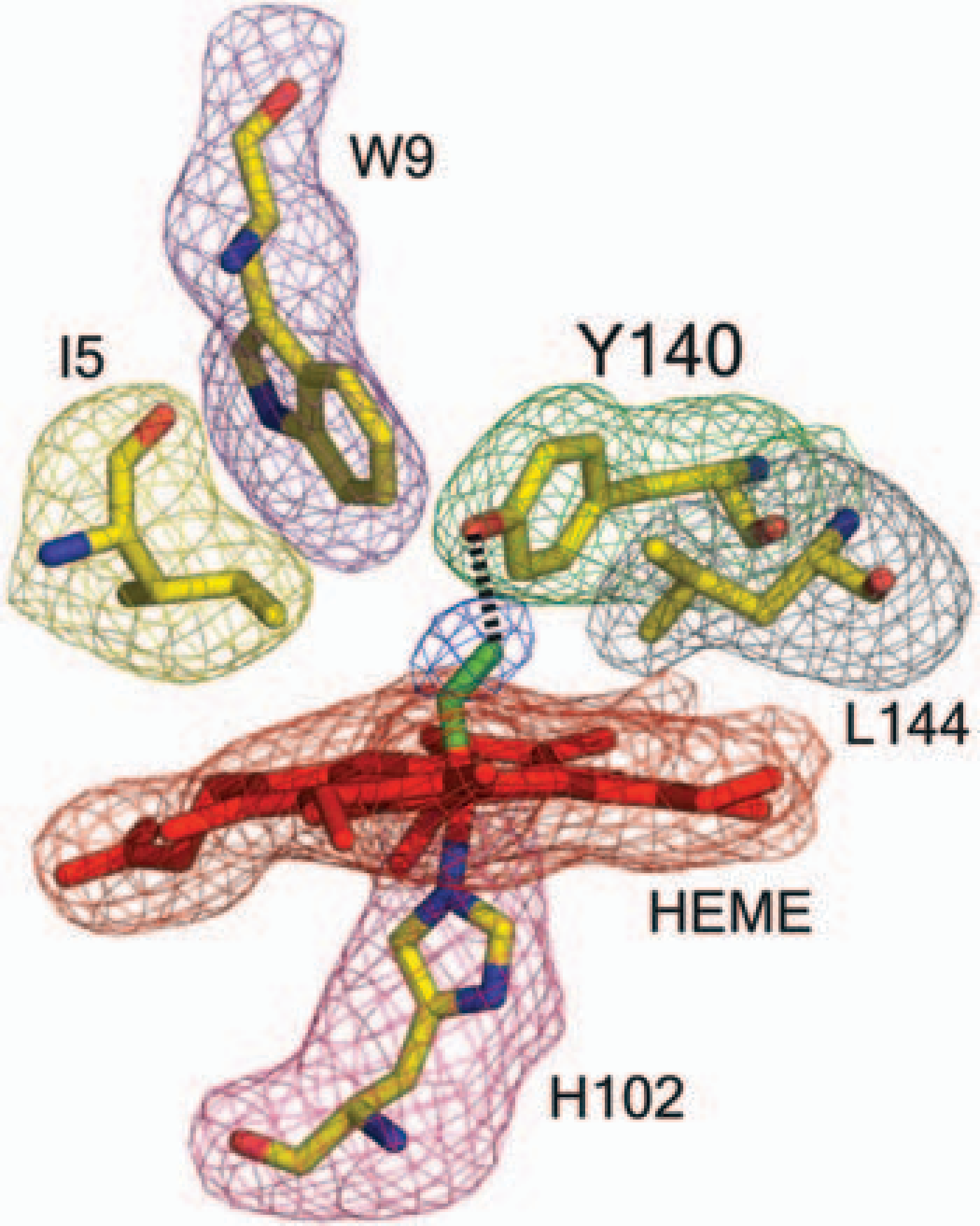
W9
I5
Y140
L144
HEME
H102